BAREKENG: Journal of Mathematics and Its Applications
June 2026 Volume 20 Issue 2 Page 1613–1626
P-ISSN: 1978-7227 E-ISSN: 2615-3017
https://doi.org/10.30598/barekengvol20iss2pp1613-1626

MATHEMATICAL MODELING OF VARICELLA TRANSMISSION USING SVEITR MODEL

Sadiyana Yaqutna Naqiya[1*], **Vina Lusiana**[2], **Achmad Abdurrazzaq**[3]

[1,2,3]*Department of Mathematics, School of Mathematics and Science,*
Republic of Indonesia Defense University
IPSC Sentul, Sukahati, Citeureup, Bogor, 16810, Indonesia.

*Corresponding author's e-mail: * **dheasadiyana@gmail.com***

Article Info

Article History:

Received: 30th June 2025
Revised: 12th August 2025
Accepted: 24th September 2025
Available Online:26th January 2026

Keywords:

Basic reproduction number;
Model development;
Numerical simulation.
SVEITR Model;
Varicella.

ABSTRACT

Varicella is a highly contagious disease with strong potential to persist endemically if not adequately controlled. This study develops an SVEITR (Susceptible–Vaccinated–Exposed–Infected–Treated–Recovered) model by extending the SVEIR and SEITR frameworks with a treatment compartment to represent individuals receiving medical care. A mathematical modeling approach was applied through differential equation formulation, equilibrium stability analysis, and computation of the basic reproduction number R_0 using the Next Generation Matrix method. The results show that $R_0 = 2.89$, confirming a high transmission potential. Numerical simulations indicate that vaccination and treatment reduce disease spread, yet waning immunity sustains a pool of susceptible individuals. These findings highlight the importance of continuous control strategies. The inclusion of a treatment compartment represents a methodological advancement, providing a more comprehensive framework for evaluating the effects of interventions on varicella transmission.

How to cite this article:

S. Y. Naqiya, V. Lusiana and A. Abdurrazzaq., "MATHEMATICAL MODELING OF VARICELLA TRANSMISSION USING SVEITR MODEL", *BAREKENG: J. Math. & App.*, vol. 20, no. 2, pp. 1613-1626, Jun, 2026.

Journal homepage: *https://ojs3.unpatti.ac.id/index.php/barekeng/*
Journal e-mail: *barekeng.math@yahoo.com; barekeng.journal@mail.unpatti.ac.id*

Research Article · Open Access

1. INTRODUCTION

Communicable diseases, such as varicella (chickenpox), have the potential to significantly impact the stability of society and the economy. The spread of communicable diseases such as varicella (chickenpox) poses a significant public health challenge, as they can disrupt social stability, economic productivity, and overall community well-being. In specific settings, including military environments, outbreaks can further impact operational readiness and erode the physical and mental resilience of defense personnel, particularly in high-density areas such as dormitories, border outposts, and guard posts. These risks highlight the importance of scientific approaches to understanding infectious disease dynamics. One such approach is the development of mathematical epidemiological models, which support data-driven decision-making for health risk mitigation strategies in both general public health and specific defense-related contexts, thereby strengthening preparedness and resilience ([1], [2], [3]).

Varicella is a highly contagious disease caused by the varicella-zoster virus (VZV), a member of the herpesviridae family. It commonly affects children, though adults who have not been infected or vaccinated remain vulnerable [4]. Transmission occurs through direct contact with vesicular fluid or airborne droplets from infected individuals [5]. Once inhaled, the virus replicates in the nasopharynx and spreads through the lymphatic and circulatory systems, infecting the skin and mucosal tissues, and resulting in fluid-filled vesicular rashes [6]. After the primary infection resolves, the virus may persist latently in nerve ganglia and reactivate as herpes zoster, especially in immunocompromised individuals [7]. Vulnerable populations include infants, pregnant women, the elderly, and those with weakened immune systems, such as cancer patients or people living with HIV [8]. In Indonesia, varicella cases are still frequently reported, particularly among unvaccinated children. Although varicella vaccines are available, their coverage remains limited, especially in densely populated areas [5]. Expanding vaccination programs and public education is crucial to reduce the incidence and preventing complications [9].

Mathematical modeling is a valuable quantitative tool for studying the spread of infectious diseases. The foundational SIR model, developed by Kermack and McKendrick in 1927, divides the population into Susceptible, Infected, and Recovered compartments and models disease dynamics through systems of differential equations [10]. Various extensions of the SIR model have been developed to accommodate more complex epidemiological phenomena. For example, the SEIR model incorporates an Exposed compartment to account for disease incubation periods [11], [12], [13], while the SVEIR model adds a Vaccinated compartment to reflect immunization efforts and waning immunity [14]. These models have been widely used to simulate different intervention strategies, including vaccination and quarantine, to evaluate their long-term impact on controlling disease spread [15], [16].

Another widely used model is the SEITR (Susceptible–Exposed–Infected–Treated–Recovered) model, which introduces a compartment for individuals undergoing medical treatment. This model is beneficial in evaluating the impact of clinical interventions such as hospitalization, antiviral therapy, or structured isolation [17], [18]. However, the SEITR model typically lacks accurate data regarding vaccine coverage and efficacy, while the SVEIR model omits treatment, making it less effective for depicting the complete progression of varicella, especially in environments with variable access to healthcare services [19].

The mathematical framework underlying these models is rooted in systems of ordinary differential equations. These equations describe continuous changes in populations over time and space, enabling prediction and simulation of epidemic behavior. The equilibrium and stability analysis of these models, based on the Jacobian matrix and eigenvalue computation, is essential for determining whether a disease will persist or die out in a population [20], [21], [22]. A central metric in this analysis is the basic reproduction number (R_0), defined as the average number of secondary infections generated by one infected individual in a fully susceptible population. When $R_0 > 1$, an outbreak is likely to spread; when $R_0 < 1$, it tends to subside [23], [24]. The Next Generation Matrix (NGM) approach is commonly used to compute R_0, particularly in multi-compartment models [25]. Several prior studies have explored the use of these models in the context of varicella and other diseases. Jose et al. in [18] applied the SVEIR model in Phuket and showed that increasing preventive measures could reduce R_0 to 0.06, significantly curbing disease spread. Musarifa et al. in [17] used the SEITR model to identify disease-free and endemic equilibrium points for varicella, showing that $R_0 > 1$ leads to endemicity, while $R_0 < 1$ indicates elimination.

This study proposes a unified SVEITR model (Susceptible–Vaccinated–Exposed–Infected–Treated–Recovered) to overcome the limitations of earlier frameworks, such as the SVEIR model, which neglects treatment effects, and the SEITR model, which does not incorporate vaccination dynamics. By integrating

both vaccination and treatment into a single framework, the SVEITR model provides a more comprehensive representation of varicella transmission and control strategies, especially in populations with variable access to healthcare and immunization programs. By integrating vaccination and treatment within a single mathematical structure, the model explicitly represents two key intervention strategies for varicella control. Vaccination is assumed to reduce the number of susceptible individuals by moving them into the vaccinated class, while accounting for waning immunity and possible vaccine failure. Treatment is represented as the transition of infected individuals into the treated compartment, which reflects clinical interventions such as antiviral therapy, hospitalization, or structured isolation aimed at accelerating recovery and reducing onward transmission. This unified framework enables analysis of how both vaccination coverage and treatment access influence disease dynamics, the basic reproduction number, and long-term control outcomes. The model aims to analyze the stability of disease transmission, compute the reproduction number, perform sensitivity analysis, and simulate the dynamics under different scenarios. The findings are expected to guide more accurate and effective strategies for varicella control, particularly in defense-related and high-density populations.

2. RESEARCH METHODS

2.1 Research Design

This study employed a quantitative-experimental research design, constructing and simulating a mathematical model to investigate the dynamics of varicella (chickenpox) transmission in Indonesia. The research expanded the SEITR (Susceptible–Exposed–Infected–Treated–Recovered) model by incorporating a vaccination compartment, resulting in the SVEITR (Susceptible–Vaccinated–Exposed–Infected–Treated–Recovered) model. Subsequent analysis included the calculation of the basic reproduction number (R0) using the Next Generation Matrix (NGM) approach and numerical simulations to explore disease behavior under various intervention scenarios.

Secondary data were utilized, gathered from literature reviews and open-access epidemiological databases, which included parameters such as transmission rate, incubation period, vaccination coverage, treatment success rates, recovery duration, and overall population exposure to varicella.

2.2 Research Timeline and Location

The methodological framework of this study consists of four main stages: (1) formulation of the SVEITR model as a system of differential equations; (2) derivation of the basic reproduction number (R_0) using the Next Generation Matrix (NGM) method; (3) equilibrium and stability analysis through Jacobian and eigenvalue computation; and (4) numerical simulations to evaluate the effects of vaccination and treatment strategies on varicella transmission dynamics.

2.3 Tools and Materials

Relevant parameter values were obtained from published epidemiological studies and official reports, as summarized in Table 1. These included infection incidence rates, transmission coefficients, vaccination coverage, and treatment outcomes, primarily sourced from Jose et al. [18] and San Martín [26]. Modeling and simulations were performed using Python.

2.4 Variables and Parameters

The model involves several key variables and parameters, categorized as follows:

Independent variable:

t: time (days).

Dependent variables

$S(t)$: susceptible individuals (persons/day);

$V(t)$: vaccinated individuals (persons/day);

$E(t)$: exposed individuals (persons/day);

$I(t)$: infected individuals (persons/day);

$T(t)$: treated individuals (persons/day);

$R(t)$: recovered individuals (persons/day).

Model parameters:

A : requirement rate;

α : vaccination rate from susceptible to vaccinated;

δ : infection rate among vaccinated individuals;

β : transmission rate from infected to susceptible;

γ : transition rate from exposed to infected;

ψ : treatment initiation rate for infected individuals;

ε_1 : recovery rate from treatment;

ε_2 : natural recovery rate without treatment;

η : immunity waning rate (recovered to susceptible);

μ : natural mortality rate.

2.5 Research Procedure

The research process began with a literature review to identify previous studies, models, and gaps related to varicella transmission. Initial models considered were SEIR, SVEIR, and SEITR, each addressing different aspects of the disease dynamics. The proposed SVEITR model integrates vaccination and treatment, overcoming the limitations of earlier models, which considered only one of these interventions.

The core steps were:

1. Model development based on differential equations representing the transitions among compartments.
2. Calculation of the basic reproduction number (R_0) using the Next Generation Matrix method to assess the outbreak potential.
3. Stability analysis of equilibrium points via the Jacobian matrix and eigenvalue analysis.
4. Numerical simulation to evaluate system behavior under different parameter settings.
5. Sensitivity analysis to identify critical parameters influencing R_0 and inform policy interventions.

2.6 Analytical Methods

2.6.1 Equilibrium Stability Analysis

The SVEITR model is represented as a system of nonlinear ordinary differential equations describing the transitions among the six compartments (S, V, E, I, T, R). The system can be expressed in the general form:

$$\frac{dx_i}{dt} = f_i(x_1, x_2, \dots, x_6), \text{for } i = 1, \dots, 6,$$

where f_i corresponds to the rate of change for each compartment.

Equilibrium points are determined by solving the system under steady-state conditions:

$$\frac{dx_i}{dt} = 0 \text{ for all compartments } x_i .$$

To analyze stability, the Jacobian matrix J is constructed as:

$$J_ij = \frac{\partial f_i}{\partial x_j} \quad (1)$$

evaluated at the equilibrium point. The eigenvalues of J determine stability: if all Re(λ) < 0, the equilibrium is locally asymptotically stable; if at least one eigenvalue has a positive fundamental part, the equilibrium is unstable.

2.6.2 Basic Reproduction Number (R_0)

The basic reproduction number was calculated using the Next Generation Matrix (NGM) approach, which separates infection dynamics into two components:

F : the rate of appearance of new infections in the exposed and infected compartments;

V : the rate of transfer into and out of these compartments (progression, recovery, natural death).

The next generation matrix is given by FV^{-1}, and the basic reproduction number is defined as:

$$R_0 = \rho(FV^{-1}) \tag{2}$$

where ρ denotes the spectral radius (dominant eigenvalue).

In the SVEITR framework, R_0 reflects the combined effects of the transmission rate (β), progression from exposed to infected (γ), treatment initiation (τ), recovery rates, and natural mortality (μ). The condition $R_0 > 1$ indicates that the infection can spread and become endemic, while $R_0 < 1$ suggests that the disease will eventually die out.

2.6.3 Sensitivity Analysis

Sensitivity analysis was conducted to identify the most influential parameters on the value of R_0. This step is crucial for informing public health strategies, as it highlights which interventions, such as increasing vaccination coverage or improving treatment initiation, would have the most significant effect in reducing transmission.

The normalized forward sensitivity index, also known as elasticity, is defined as:

$$ES_p^{R_0} = \left(\frac{\partial R_0}{\partial p}\right) * \left(\frac{p}{R_0}\right) \tag{3}$$

where p is a parameter of interest. We have two possibilities for elasticity which are a positive elasticity means that increasing p raises R_0, and a negative elasticity means that increasing p reduces R_0.

3. RESULTS AND DISCUSSION

3.1 Model Assumptions and Construction

The SVEITR model developed in this study divides the total population into six mutually exclusive compartments: Susceptible (S), Vaccinated (V), Exposed (E), Infected (I), Treated (T), and Recovered (R). These compartments reflect the key stages of varicella progression and control within a population. The model is constructed under the following assumptions: (1) the characteristics of varicella are consistent across countries, irrespective of climate differences [27]; (2) the disease has a defined incubation period during which exposed individuals do not transmit the virus; (3) both vaccinated and recovered individuals may lose immunity and return to the susceptible class; and (4) natural birth and death rates are constant across compartments.

Based on these assumptions, a system of ordinary differential equations describes the temporal dynamics of each compartment. The flow diagram of transmission becomes the following model equations:

$$\frac{dS}{dt} = A + \delta V + \eta T - \alpha S - \beta SI - \mu S, \tag{4}$$

$$\frac{dV}{dt} = \alpha S - (1-\delta)\beta VI - \delta V - \mu V, \tag{5}$$

$$\frac{dE}{dt} = \beta SI + (1-\delta)\beta VI - \gamma E - \mu E, \tag{6}$$

$$\frac{dI}{dt} = \gamma E - \psi I - \varepsilon_2 I - \mu I, \tag{7}$$

$$\frac{dT}{dt} = \psi I - \varepsilon_1 T - \mu T, \tag{8}$$

$$\frac{dR}{dt} = \varepsilon_2 I + \varepsilon_1 T - \eta R - \mu R. \tag{9}$$

These equations account for susceptible, vaccinated, exposed, infected, treated, and naturally recovered.

3.2 Equilibrium Analysis

Two equilibrium points are considered: the Disease-Free Equilibrium (DFE) and the Endemic Equilibrium (EE). The DFE is determined by setting $E = I = T = R = 0$, indicating no infection within the population. Solving the equilibrium equations yields:

$$S^* = \frac{A(\delta + \mu)}{\mu(\alpha + \delta + \mu)}, \qquad V^* = \frac{A\alpha}{\mu(\alpha + \delta + \mu)}. \tag{10}$$

Thus, the DFE point is:

$$(S^*, V^*, 0,0,0,0).$$

The endemic equilibrium (EE), which reflects persistent disease in the population, occurs when $E^*, I^*, T^*, R^* > 0$. To obtain the EE, the system of differential equations is set equal to zero $\left(\frac{dS}{dt} = \frac{dV}{dt} = \frac{dE}{dt} = \frac{dI}{dt} = \frac{dT}{dt} = \frac{dR}{dt} = 0\right)$. This results in a system of nonlinear algebraic equations that links the steady-state values of each compartment. Specifically, the balance equations are solved sequentially: the susceptible equilibrium S^* is obtained by equating the inflow (births and loss of immunity) with the outflow (infection, vaccination, and natural death); the vaccinated equilibrium V^* follows from the transition from susceptible to vaccinated; the exposed equilibrium E^* is expressed in terms of S^*, V^*, and I^*; the infected equilibrium I^* is derived from the progression of exposed individuals; and finally the treated equilibrium T^* is determined by the treatment initiation rate. Although the exact closed-form solutions are algebraically complex, the resulting system can be summarized as:

$$S^* = \frac{A + \delta V^* + \eta R^*}{\alpha + \beta I^* + \mu}, \tag{11}$$

$$V^* = \frac{\alpha S^*}{(1-\delta)\beta + \delta + \mu}, \tag{12}$$

$$E^* = \frac{\beta S^* I^* + (1-\delta)\beta V^*}{\gamma + \mu}, \tag{13}$$

$$I^* = \frac{\gamma E^*}{1 + \mu}, \tag{14}$$

$$T^* = \frac{(1-\psi) I^*}{\varepsilon + \mu}, \tag{15}$$

$$R^* = \frac{\psi I^* + \varepsilon T^*}{\eta + \mu}. \tag{16}$$

These equations provide the endemic equilibrium values in terms of the model parameters. While no single formula describes them, the models can be solved numerically to investigate varicella persistence across various intervention strategies.

3.3 Stability Analysis

To determine the local stability of the DFE, the Jacobian matrix was constructed and evaluated at the equilibrium point. The value of the Jacobian matrix can be obtained from:

$$J = \begin{pmatrix} -\alpha-\mu & \delta & 0 & -\beta S^* & 0 & \eta \\ \alpha & -\delta-\mu & 0 & -(1-\delta)\beta V^* & 0 & 0 \\ 0 & 0 & -\gamma-\mu & \beta S^* + (1-\delta)\beta V^* & 0 & 0 \\ 0 & 0 & \gamma & -\mu-\psi-\varepsilon_2 & 0 & 0 \\ 0 & 0 & 0 & \psi & -\varepsilon_1-\mu & 0 \\ 0 & 0 & 0 & \varepsilon_2 & \varepsilon_1 & -\eta-\mu \end{pmatrix}.$$

The characteristic eigenvalues obtained were:

$$\lambda_1 = -\alpha - \delta - \mu = -0.03928694;$$
$$\lambda_2 = -\varepsilon_1 - \mu = -0.03701694;$$
$$\lambda_3 = -\eta - \mu = -0.00044594;$$
$$\lambda_4 = -\mu = -0.00001694;$$
$$\lambda_{5,6} = -\frac{\gamma + 2\psi + \varepsilon_2 + 2\mu}{2} \pm \frac{1}{2}\sqrt{(\gamma - (\psi + \varepsilon_2))^2 + 4\gamma\kappa};$$
$$\lambda_5 = -0.32155402965;$$
$$\lambda_6 = -0.02093373035;$$

Since all eigenvalues have negative real parts, the DFE is locally asymptotically stable, confirming that the infection dies out in the long run when $R_0 < 1$.

Table 1. Parameter Value

Variabel	Value	Source
A	9	[18]
α	0.00504	[18]
δ	0.03423	[18]
β	0.000010778	[18]
γ	0.00242	[18]
ψ	0.075	[18]
ε_1	0.037	[18]
ε_2	0,04	[18]
η	0.000429	[18]
μ	0.00001694	[18]

3.4 Basic Reproduction Number R_0

Using the Next Generation Matrix (NGM) method, the basic reproduction number was derived by decomposing the infection matrix F and the transition matrix V that are

$$F = \begin{pmatrix} 0 & \beta S + (1-\delta)\beta V & 0 \\ 0 & 0 & 0 \\ 0 & 0 & 0 \end{pmatrix}, \quad (17)$$

and

$$V = \begin{pmatrix} \gamma + \mu & 0 & 0 \\ -\gamma & \mu + \psi + \varepsilon_2 & 0 \\ 0 & -\psi & \mu + \varepsilon_1 \end{pmatrix}.$$

The final analytical expression for R_0 is:

$$R_0 = \frac{\gamma\beta A[(\delta+\mu) + (1-\delta)\alpha]}{\mu(\alpha+\delta+\mu)(\gamma+\mu)(\psi+\varepsilon_2+\mu)}. \quad (18)$$

Substituting the parameter values yields:

$$R_0 = 2.89. \quad (19)$$

This value, significantly greater than 1, indicates that varicella has a strong potential to spread within the population, confirming that the disease remains endemic under current conditions.

3.5 Sensitivity Analysis

Sensitivity analysis was carried out to assess how changes in the main parameters affect R_0according to the steps in (3) so that the values obtained are as in Table 2:

Table 2. Sensitivity analysis parameters against R_0 value

Parameter	Description	Elasticity $ES_p^{\{R_0\}}$	Interpretation
A	Recruitment/birth rate	+1.000	A 1% increase in AA leads to a 1% increase in R_0.
β	Transmission rate	+1.000	A 1% increase in β leads to a 1% increase in R_0.
γ	Progression rate (E → I)	+0.007	Very small effect; almost no change in R_0 .
α	Vaccination rate	−0.004	Slightly reduces R_0 when α increases.
δ	Vaccine failure rate	−0.001	Negligible effect on R_0.
ψ	Treatment initiation rate	−0.652	Substantially reduces R_0; higher ψ leads to stronger control.
ε2	Natural recovery rate (from I)	−0.348	Moderate reduction of R_0 as ε2 increases.
μ	Natural death rate	−1.010	A 1% increase in μ reduces R_0 by ≈1%.

In this sensitivity analysis, the author only simulates numerically the $\alpha, \beta, \delta,$ and ψ parameters numerically because their significant influence on the Ro value can be seen in the following simulation figure:

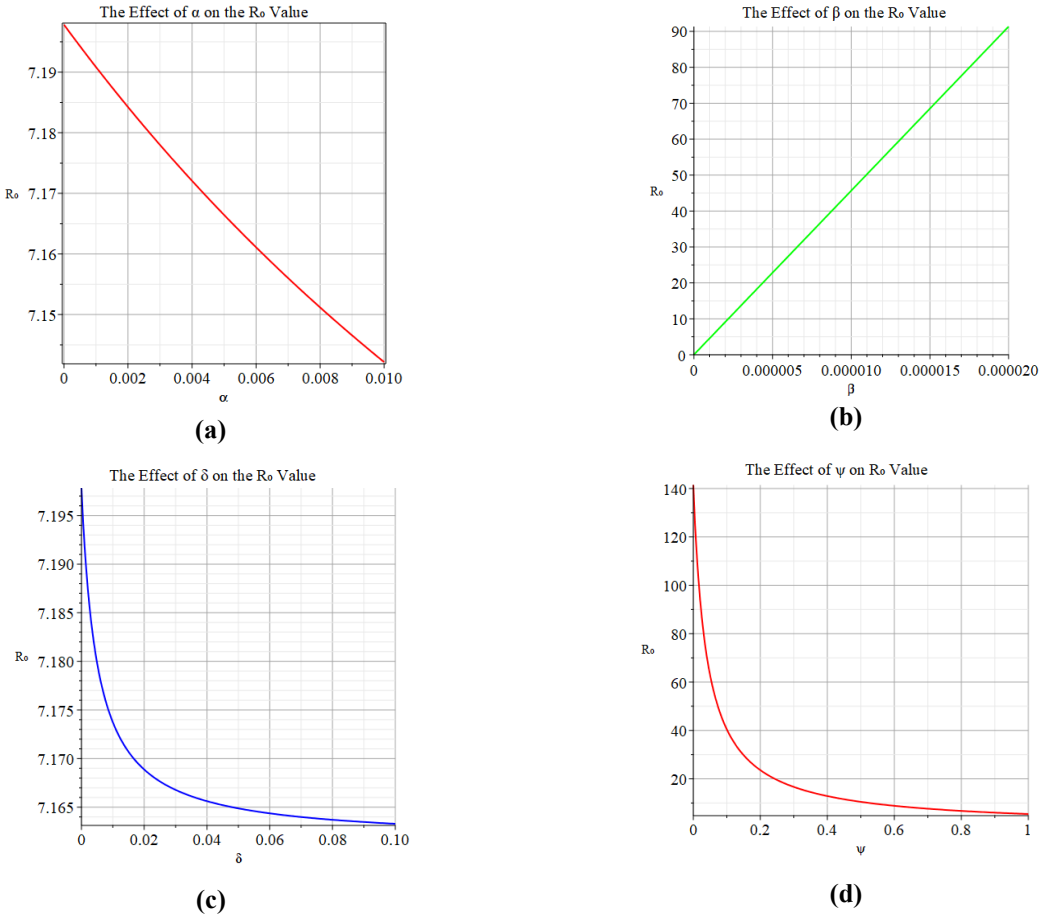

Figure 1. Basic Reproduction Number Against Parameters (a). α (b). β (c). δ and (d). ψ

The simulation results Fig. 1 show that:

1. Increasing the vaccination rate αdecreases R_0 steadily.
2. Increasing the transmission rate β increases R_0 linearly.
3. Increasing the vaccine failure rate δ decreases R_0, though with diminishing returns.
4. Increasing the treatment rate ψ also leads to a reduction in R_0.

These results highlight the importance of increasing vaccination coverage and improving treatment access to control the spread of varicella.

3.6 Numerical Simulation

The numerical simulation shown below is the change in each compartment against time starting from susceptible, vaccinated, exposed, infected, treated, and recovered in a 10,000-day period using the initial condition:

$$S(0) = 463.129, V(0) = 68.157, E(0) = 10, I(0) = 5, T(0) = 0, R(0) = 0. \quad (20)$$

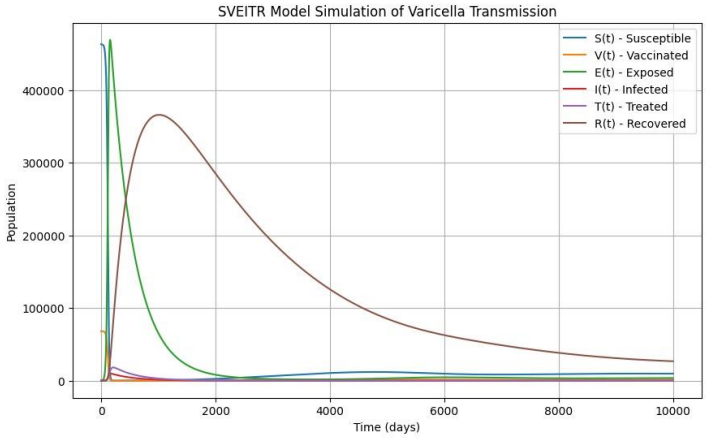

Figure 2. Population Dynamics of Varicella Disease Spread Over Time

The simulation results Fig. 2 show that:

1. The susceptible population decreases sharply at the beginning due to both infection and vaccination, and later stabilizes at a lower level as transitions with other compartments balance out.
2. The vaccinated population rises significantly in the early phase, reflecting intensive vaccination, but then drops as immunity wanes and some individuals move to the exposed or other compartments.
3. The exposed population shows an early spike (around day 200–300), capturing the initial rapid spread of varicella, and then gradually declines to near zero.
4. The infected and treated populations remain at relatively low levels compared to other compartments, indicating that although infection persists, it is controlled through treatment and recovery.
5. The recovered population increases consistently and becomes the dominant group in the long run, signifying that most individuals eventually gain immunity after infection or treatment.

3.6.1 Susceptible Compartment

Fig. 3 illustrates the effect of parameters α, β, δ, and η on the dynamics of the susceptible population $S(t)$ in the SVEITR varicella model. An increase in the vaccination rate (α) and transmission rate (β) significantly accelerates the decline of $S(t)$, due to more individuals being vaccinated and infected, respectively. In contrast, changes in the vaccine failure rate (δ) and immunity loss rate (η) have minimal impact on the susceptible curve, indicating their relatively minor influence over the simulation period.

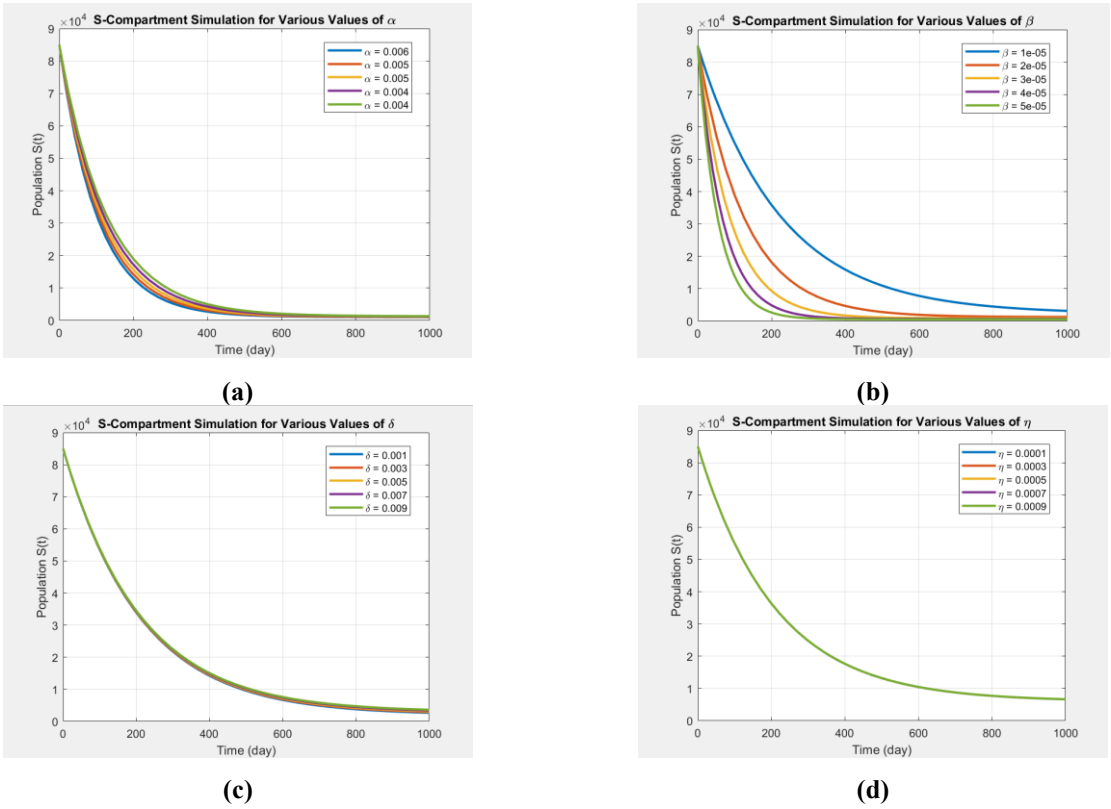

Figure 3. Susceptible Compartment Simulation against Parameters (a). α (b). β (c). δ (d). η

3.6.2 Vaccinated Compartment

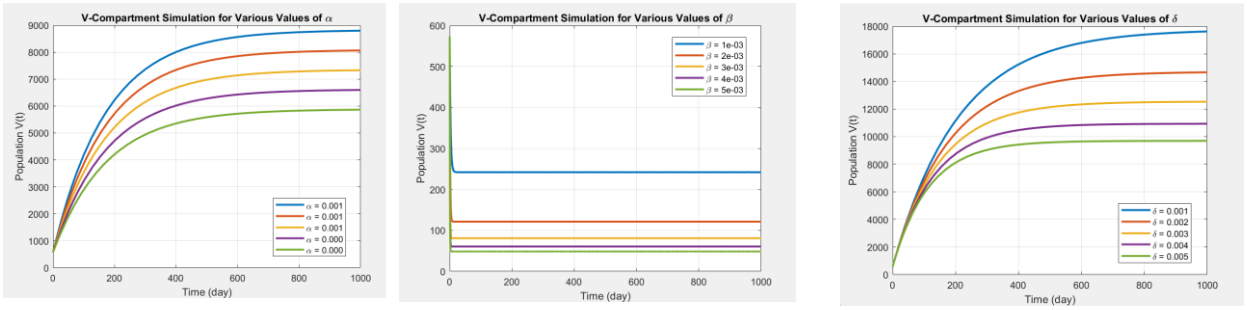

Figure 4. Vaccinated Compartment Simulation against Parameters (a). α (b). β (c). δ

Fig. 4 illustrates the dynamics of the vaccinated population $V(t)$ in response to variations in parameters $\alpha, \beta,$ and δ within the $SVEITR$ model. Subfigure (a) demonstrates that a higher vaccination rate (α) significantly increases the number of vaccinated individuals over time, reflecting broader immunization coverage. Subfigure (b) reveals that a higher transmission rate (β) reduces $V(t)$, as vaccinated individuals become exposed more quickly due to increased infection risk. In subfigure (c), an increase in vaccine failure rate (δ) leads to a long-term decline in the vaccinated population, as more individuals lose vaccine-conferred protection.

3.6.3 Exposed Compartment

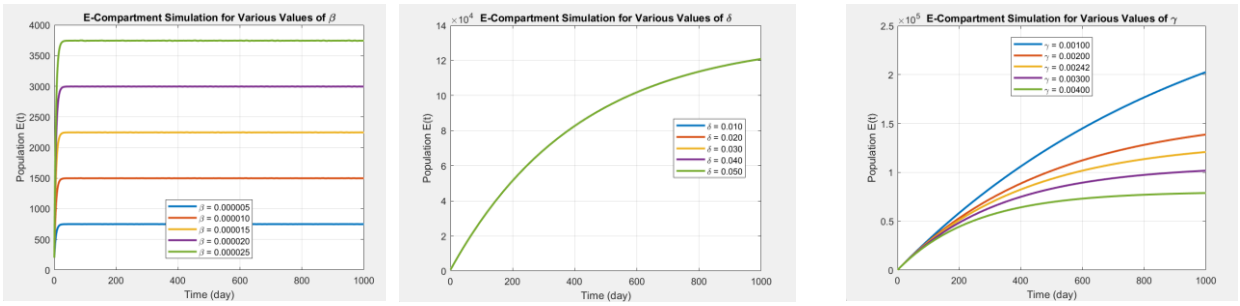

(a) **(b)** **(c)**

Figure 5. Exposed Compartment Simulation against Parameters (a). β (b). δ (c). γ

Fig. 5 illustrates the dynamics of the exposed population $E(t)$ under variations in parameters β, δ, and γ in the $SVEITR$ model. In subfigure (a), a higher transmission rate (β) significantly increases the number of exposed individuals, indicating greater infection risk. Subfigure (b) shows that increased vaccine effectiveness (higher δ) drastically reduces the exposed population, demonstrating the vaccine's role in lowering exposure. In subfigure (c), a higher transition rate to the infectious class (γ) decreases $E(t)$, as individuals move more quickly from the exposed to the infectious stage, shortening their time in the E compartment.

3.6.4 Infected Compartment

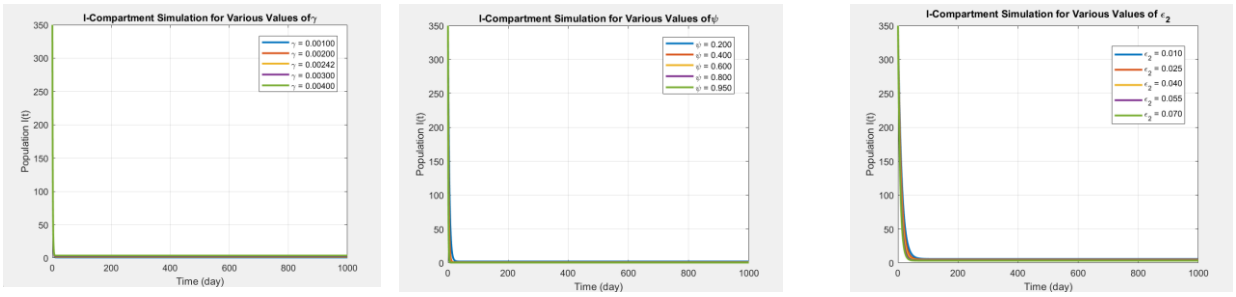

(a) **(b)** **(c)**

Figure 6. Infected Compartment Simulation against Parameters (a). γ (b). ψ (c). ε_2

Fig. 6 displays the dynamics of the infectious compartment $I(t)$ in response to variations in parameters γ, ψ, and ε_2. An increase in the transition rate γ from exposed to infectious accelerates the initial rise of the contagious population, indicating γ's influence on how quickly individuals become infectious, although it does not significantly alter the final value. Subfigure (b) shows that changes in ψ (treatment initiation rate) have minimal impact on the final size of $I(t)$, as all curves quickly converge to a very low level. Likewise, variations in ε_2 (natural recovery rate) exert little influence on $I(t)$, suggesting that transitions occurring after infection do not substantially affect the infectious population.

3.6.5 Treated Compartment

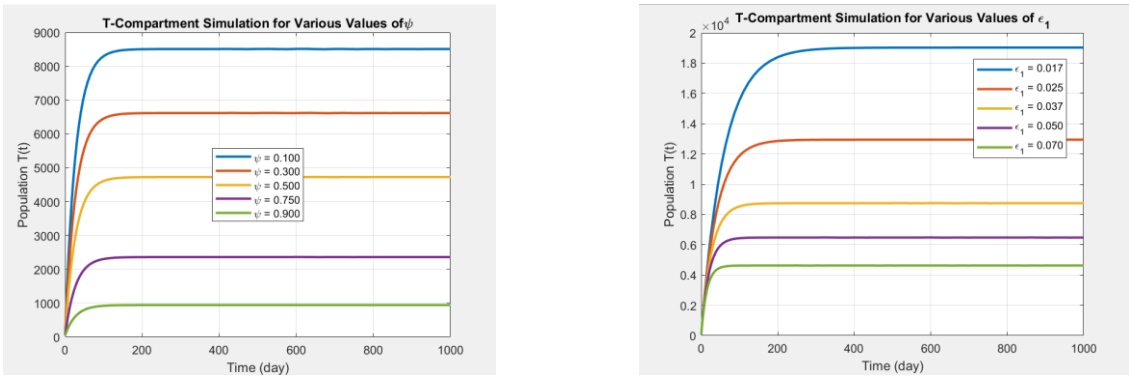

(a) **(b)**

Figure 7. Treated Compartment Simulation against Parameters (a). ψ (b). ε_1

Fig. 7 illustrates the simulation of the treated compartment $T(t)$ in response to variations in parameters ψ and ε_1. In subfigure (a), increasing the treatment rate ψ leads to a decline in $T(t)$, which is reasonable since more individuals recover directly without entering the treatment phase, thus reducing the burden on this compartment. Conversely, in subfigure (b), a higher value of ε_1 significantly increases the treated population, as more individuals transition from the infectious compartment to treatment, resulting in greater accumulation within $T(t)$.

Some conclusions can be drawn from these additional simulations. These simulations revealed:

1. α and β significantly affect susceptible and vaccinated populations.
2. δ, γ and ψ strongly influence the dynamics of exposed and infected compartments.
3. Treatment dynamics are sensitive to ψ and ε_1, which regulate flow into and out of the treated class.

Overall, the model confirms that improving vaccination coverage and accelerating treatment response are effective strategies for reducing the spread of varicella and lowering the basic reproduction number.

4. CONCLUSION

This study successfully developed a mathematical epidemiological model of varicella transmission by integrating and extending two previous models—$SVEIR$ and $SEITR$—into a comprehensive $SVEITR$ framework. The model incorporates six compartments: Susceptible (S), Vaccinated (V), Exposed (E), Infected (I), Treated (T), and Recovered (R). The resulting system of differential equations captures the essential dynamics of varicella transmission under vaccination and treatment interventions. The analysis shows that:

1. The basic reproduction number R_0 was computed numerically and found to be 2.89, indicating a high level of contagiousness. This value implies that, in a completely susceptible population, each infected individual can transmit the disease to nearly three others, suggesting that varicella remains endemic under current conditions.
2. The numerical simulations further revealed the trajectory of disease spread over a 10,000-day period, demonstrating that interventions such as vaccination and medical treatment substantially reduce the number of infections and accelerate population recovery.
3. Sensitivity analysis emphasized the critical role of the vaccination rate (α) and vaccine failure rate (δ) in modulating the value of R_0. Increasing α and improving vaccine effectiveness (i.e., reducing δ) significantly reduced disease transmission, validating the importance of robust immunization programs.

However, this study has several limitations. The model assumes homogeneous population mixing and constant parameter values, so it may not fully reflect the complexity of real-world transmission dynamics. Furthermore, demographic heterogeneity, spatial mobility, stochastic effects, and variations in vaccine effectiveness have not been considered. These factors have the potential to impact the accuracy of the model's predictions.

Author Contributions

Sadiyana Yaqutna Naqiya: Conceptualization, Data Curation, Formal Analysis, Methodology, Visualization, Writing - Original Draft. Vina Lusiana: Supervision, Conceptualization, Methodology, Validation, Writing - Review and Editing. Achmad Abdurrazzaq: Supervision, Validation, Writing - Review and Editing. All authors contributed to the interpretation of the results, reviewed the manuscript, and approved the final version for publication.

Funding Statement

This research received no specific grant from any funding agency in the public, commercial, or not-for-profit sectors.

Acknowledgment

The authors gratefully acknowledge the Republic of Indonesia Defense University for its continuous support and provision of research facilities that enabled this study. Special thanks are extended to the Department of Mathematics, School of Mathematics and Science, for valuable guidance and academic assistance throughout the research process. The authors express sincere appreciation to Galih Pradananta for carefully reviewing the article prior to submission and providing valuable suggestions for improving the narrative structure and figure presentation.

Declarations

Competing interest. The authors declare no competing interest.

Declaration of Generative AI and AI-assisted technologies

Generative AI tools (e.g., ChatGPT) were used solely for language refinement (grammar, spelling, and clarity). The scientific content, analysis, interpretation, and conclusions were developed entirely by the authors. The authors reviewed and approved all final text.

REFERENCES

[1] J. R. Duncan, C. T. Witkop, B. J. Webber, and A. A. Costello, "VARICELLA SEROEPIDEMIOLOGY IN UNITED STATES AIR FORCE RECRUITS: A RETROSPECTIVE COHORT STUDY COMPARING IMMUNOGENICITY OF VARICELLA VACCINATION AND NATURAL INFECTION," *Vaccine*, vol. 35, no. 18, pp. 2351–2357, Apr. 2017, doi: https://doi.org/10.1016/j.vaccine.2017.03.054.

[2] P. Karki *et al.*, "AN OUTBREAK INVESTIGATION OF VARICELLA ZOSTER AMONG MALE MILITARY PERSONNEL IN A MILITARY TRAINING CENTRE," *J. Nepal Med. Assoc.*, vol. 60, no. 249, pp. 469–472, May 2022, doi: https://doi.org/10.31729/jnma.7440.

[3] S. Patrikar *et al.*, "HEALTH TECHNOLOGY ASSESSMENT OF VARICELLA VACCINE IN THE ARMED FORCES," *Med. J. Armed Forces India*, vol. 78, no. 2, pp. 213–220, Apr. 2022, doi: https://doi.org/10.1016/j.mjafi.2021.06.010.

[4] G. Zhu *et al.*, "CHICKENPOX AND MULTIPLE SCLEROSIS: A MENDELIAN RANDOMIZATION STUDY," *J. Med. Virol.*, vol. 95, no. 1, p. 28315, Jan. 2023, doi: https://doi.org/10.1002/jmv.28315.

[5] A. Patil, M. Goldust, and U. Wollina, "HERPES ZOSTER: A REVIEW OF CLINICAL MANIFESTATIONS AND MANAGEMENT," *Viruses*, vol. 14, no. 2, p. 192, Jan. 2022, doi: https://doi.org/10.3390/v14020192.

[6] A. A. Gershon *et al.*, "VARICELLA ZOSTER VIRUS INFECTION," *Nat. Rev. Dis. Prim.*, vol. 1, no. 1, p. 15016, Jul. 2015, doi: https://doi.org/10.1038/nrdp.2015.16.

[7] L. Laemmle, R. S. Goldstein, and P. R. Kinchington, "MODELING VARICELLA ZOSTER VIRUS PERSISTENCE AND REACTIVATION – CLOSER TO RESOLVING A PERPLEXING PERSISTENT STATE," *Front. Microbiol.*, vol. 10, no. 2019, p. 1634, Jul. 2019, doi: https://doi.org/10.3389/fmicb.2019.01634.

[8] C. Lo Presti, C. Curti, M. Montana, C. Bornet, and P. Vanelle, "CHICKENPOX: AN UPDATE," *Médecine Mal. Infect.*, vol. 49, no. 1, pp. 1–8, Feb. 2019, doi: https://doi.org/10.1016/j.medmal.2018.04.395.

[9] B. Hao *et al.*, "EFFICACY, SAFETY AND IMMUNOGENICITY OF LIVE ATTENUATED VARICELLA VACCINE IN HEALTHY CHILDREN IN CHINA: DOUBLE-BLIND, RANDOMIZED, PLACEBO-CONTROLLED CLINICAL TRIAL," *Clin. Microbiol. Infect.*, vol. 25, no. 8, pp. 1026–1031, Aug. 2019, doi: https://doi.org/10.1016/j.cmi.2018.12.033.

[10] V. Capasso and G. Serio, "A GENERALIZATION OF THE KERMACK-MCKENDRICK DETERMINISTIC EPIDEMIC MODEL," *Math. Biosci.*, vol. 42, no. 1–2, pp. 43–61, Nov. 1978, doi: https://doi.org/10.1016/0025-5564(78)90006-8.

[11] M. Fošnarič, T. Kamenšek, J. Žganec Gros, and J. Žibert, "EXTENDED COMPARTMENTAL MODEL FOR MODELING COVID-19 EPIDEMIC IN SLOVENIA," *Sci. Rep.*, vol. 12, no. 1, p. 16916, Oct. 2022, doi: https://doi.org/10.1038/s41598-022-21612-7.

[12] H. Wang, X. Qiu, J. Yang, Q. Li, X. Tan, and J. Huang, "NEURAL-SEIR: A FLEXIBLE DATA-DRIVEN FRAMEWORK FOR PRECISE PREDICTION OF EPIDEMIC DISEASE," *Math. Biosci. Eng.*, vol. 20, no. 9, pp. 16807–16823, 2023, doi: https://doi.org/10.3934/mbe.2023749.

[13] I. N. Kiselev, I. R. Akberdin, and F. A. Kolpakov, "DELAY-DIFFERENTIAL SEIR MODELING FOR IMPROVED MODELLING OF INFECTION DYNAMICS," *Sci. Rep.*, vol. 13, no. 1, p. 13439, Aug. 2023, doi: https://doi.org/10.1038/s41598-023-40008-9.

[14] M. El Hajji and A. H. Albargi, "A MATHEMATICAL INVESTIGATION OF AN 'SVEIR' EPIDEMIC MODEL FOR THE MEASLES TRANSMISSION," *Math. Biosci. Eng.*, vol. 19, no. 3, pp. 2853–2875, 2022, doi: https://doi.org/10.3934/mbe.2022131.

[15] M. Irwan, Wahidah Alwi, and Susrianti, "SIMULASI MODEL SVIR (SUSCEPTIBLE, VACCINATED, INFECTED, RECOVERED) PADA KASUS COVID-19," *J. MSA (Mat. dan Stat. serta Apl.*, vol. 10, no. 2, pp. 104–108, Dec. 2022, doi: https://doi.org/10.24252/msa.v10i2.33657.

[16] S. P. Sari and E. Arfi, "ANALISIS DINAMIK MODEL SIR PADA KASUS PENYEBARAN PENYAKIT CORONA VIRUS DISEASE-19 (COVID-19)," *Indones. J. Appl. Math.*, vol. 1, no. 2, p. 61, May 2021, doi:

https://doi.org/10.35472/indojam.v1i2.354.

[17] Musarifa, Hikmah, and Fardinah, "ANALISIS MODEL MATEMATIKA SEITR PADA PENYAKIT CACAR AIR," *J. Math. Theory Appl.*, vol. 3, no. 2, pp. 45–52, Dec. 2021, doi: https://doi.org/10.31605/jomta.v3i2.1372.

[18] S. A. Jose, R. Raja, J. Dianavinnarasi, D. Baleanu, and A. Jirawattanapanit, "MATHEMATICAL MODELING OF CHICKENPOX IN PHUKET: EFFICACY OF PRECAUTIONARY MEASURES AND BIFURCATION ANALYSIS," *Biomed. Signal Process. Control*, vol. 84, no. february, p. 104714, Jul. 2023, doi: https://doi.org/10.1016/j.bspc.2023.104714.

[19] N. Izzati and A. Andriani, "KENDALI OPTIMAL PADA MODEL PENYEBARAN PENYAKIT DIFTERI DENGAN TINGKAT IMUNITAS ALAMI PADA INDIVIDU TERPAPAR," *J. Ilm. Mat. DAN Terap.*, vol. 18, no. 1, pp. 1–10, Jun. 2021, doi: https://doi.org/10.22487/2540766X.2021.v18.i1.15339.

[20] M ZULKIFLI WARLI, "ANALISIS KESTABILAN MODEL PERTUMBUHAN SEL KANKER DENGAN TERAPI GEN ONYX P53," *Prox. J. Penelit. Mat. dan Pendidik. Mat.*, vol. 4, no. 2, pp. 1–11, Aug. 2021, doi: https://doi.org/10.30605/proximal.v4i2.1244.

[21] M. Jannah, M. Ahsar Karim, and Y. Yulida, "ANALISIS KESTABILAN MODEL SEIR UNTUK PENYEBARAN COVID-19 DENGAN PARAMETER VAKSINASI," *BAREKENG J. Ilmu Mat. dan Terap.*, vol. 15, no. 3, pp. 535–542, Sep. 2021, doi: https://doi.org/10.30598/barekengvol15iss3pp535-542.

[22] P. Gonçalves, "BEHAVIOR MODES, PATHWAYS AND OVERALL TRAJECTORIES: EIGENVECTOR AND EIGENVALUE ANALYSIS OF DYNAMIC SYSTEMS," *Syst. Dyn. Rev.*, vol. 25, no. 1, pp. 35–62, Jan. 2009, doi: https://doi.org/10.1002/sdr.414.

[23] V. LUSIANA, "PERMODELAN MATEMATIKA TRANSMISI KO-INFEKSI TUBERKULOSIS PADA KOMUNITAS HIV," *Knowl. J. Inov. Has. Penelit. dan Pengemb.*, vol. 2, no. 2, pp. 146–156, Aug. 2022, doi: https://doi.org/10.51878/knowledge.v2i2.1409.

[24] S. Dharmaratne, S. Sudaraka, I. Abeyagunawardena, K. Manchanayake, M. Kothalawala, and W. Gunathunga, "ESTIMATION OF THE BASIC REPRODUCTION NUMBER (R0) FOR THE NOVEL CORONAVIRUS DISEASE IN SRI LANKA," *Virol. J.*, vol. 17, no. 1, p. 144, Dec. 2020, doi: https://doi.org/10.1186/s12985-020-01411-0.

[25] S. M. A. Rahman and X. Zou, "MODELLING THE IMPACT OF VACCINATION ON INFECTIOUS DISEASES DYNAMICS," *J. Biol. Dyn.*, vol. 9, no. sup1, pp. 307–320, Jun. 2015, doi: https://doi.org/10.1080/17513758.2014.986545.

[26] P. San Martin *et al.*, "SYSTEMATIC LITERATURE REVIEW OF HERPES ZOSTER DISEASE BURDEN IN SOUTHEAST ASIA," *Infect. Dis. Ther.*, vol. 12, no. 6, pp. 1553–1578, Jun. 2023, doi: https://doi.org/10.1007/s40121-023-00822-0.

[27] T. Cheng, Y. Bai, X. Sun, Y. Ji, F. Zhang, and X. Li, "EPIDEMIOLOGICAL ANALYSIS OF VARICELLA IN DALIAN FROM 2009 TO 2019 AND APPLICATION OF THREE KINDS OF MODEL IN PREDICTION PREVALENCE OF VARICELLA," *BMC Public Health*, vol. 22, no. 1, p. 678, Dec. 2022, doi: https://doi.org/10.1186/s12889-022-12898-3.